Revision Submitted to Optometry & Vision Science

June 8, 1999

Non-Linear Alteration of Transient Vergence Dynamics After Sustained Convergence*

Saumil S. Patel, Ph.D.

Bai-Chuan Jiang, Ph.D.

University of Houston, College of Optometry, Houston, Texas

Janis M. White, O.D., Ph.D.

Veterans New Jersey Health Care System, East Orange, New Jersey

and

Haluk Ogmen, Ph.D.

University of Houston, Cullen College of Engineering

* Including 2 tables and 4 figures

Parts of this study were presented as a poster at the 1995 ARVO annual meeting in Ft. Lauderdale.

ABSTRACT

Background. Adaptation models of the horizontal disparity vergence system assume a non-adaptable transient component. They also predict identical post-adaptation dynamics during convergence and divergence movements. *Method*. To test the adaptation property of the *transient* component, a set of experiments are performed in which closed-loop vergence dynamics measured before and after sustained convergence are compared, primarily by comparing the peak vergence velocity, occurrence time of peak vergence velocity and steady-state vergence posture. Vergence dynamics after durations of 30, 60 and 90 secs of sustained convergence are compared to those after a control duration of 5 sec. *Results*. The peak divergence velocity is reduced by about 25% within 30 secs of sustained vergence. However, the peak convergence velocity is unchanged for all the exposure durations. Additionally, for all durations, the peak divergence velocity is significantly higher than peak convergence velocity. In contrast to peak velocities, the occurrence time of peak convergence and divergence velocity did not differ significantly and remained unchanged for all durations. *Conclusions*. It is shown that the transient component is adaptable. Furthermore, the adaptation is direction dependent and affects divergence and convergence dynamics differently, thereby suggesting involvement of separate pathways for convergence and divergence in the vergence sensorimotor control.

Key words: divergence, oculomotor, vergence adaptation, model, accommodation

INTRODUCTION

The vergence system controls disjunctive eye movements, permitting binocular fixation of targets at various distances. It is stimulated by many cues such as retinal disparity, defocus blur and proximal cues to depth. In addition, there is a tonic vergence level, thought of as the resting or baseline level of the vergence system. It determines the intermediate resting state of vergence, or that state when there is no visual stimulus, accommodative activity or voluntary effort to modify vergence.[1] The tonic vergence is usually measured as the vergence posture at a pre-defined time (~40 sec)[2] after a previously viewed binocular stimulus is removed, generally by introduction of darkness[3] or by occlusion of one eye. Because vergence eye movements are believed to be accomplished by the interaction of convergence and divergence activities,[4,5] the tonic vergence can be conceptualized as an equilibrium between these two mechanisms when the sensory stimulus to the vergence system is absent. Therefore, the tonic vergence, which is generally represented by a scalar variable, must be carefully observed and interpreted since divergence and convergence are active dynamic processes. In the entire paper, convergence and divergence are defined with respect to a current vergence posture.

After sustained viewing of a binocular stimulus, the tonic vergence of a given individual is modified, a process called vergence adaptation. In this paper, the word *adaptation* refers to a change in vergence dynamics that is dependent on the duration of binocular stimulus exposure, and is used synonymously with the consequence of sustained convergence exposure. When the binocular stimulus is eliminated after the adaptation (by introduction of darkness), vergence posture decays, fairly rapidly at first and then more slowly (bi-phasic decay), back to its pre-task level.[6,7] Generally, the rate of this decay is smaller as the duration of the vergence stimulus is increased,[6,8-11] hence the tonic vergence, which is

measured at a pre-defined time, is elevated. The modification of tonic vergence has been the focus of most vergence adaptation studies.[7,12-20] The tonic vergence modification is also known as phoria adaptation. Current models of vergence adaptation have incorporated plasticity of tonic vergence in the sustained component of a transient -sustained (phasic-tonic) architecture.[6,21,22] In addition, the models assume a parallel non-adaptable transient component that responds to rapid changes in ocular vergence demand. The initial fast phase in the bi-phasic decay of vergence posture in darkness is attributed to the non-adaptable transient component.[6]

Although, the models by Schor[6,22] and Hung[21] both incorporate tonic vergence plasticity in their sustained components, the suggested underlying neural mechanisms are different. Schor's model suggests a recruitment mechanism that could be achieved by a continuum of threshold units that are an order of magnitude slower than the units in the transient component. A 'unit' is defined as a collection of neurons having similar functional properties. As vergence exposure duration is increased at a given posture, more units get recruited thereby increasing the output of the sustained component, and reducing the drive from the transient component. In contrast, Hung's model suggests a variable time-constant mechanism in which units increase their time-constants proportionally to the exposure. In Schor's model, the sustained component is driven by the transient component while in Hung's model, the signals to each component are not explicitly shown. In Hung's model the transient component is eliminated from the actual model used to characterize vergence adaptation due to the assumption that it is non-adaptable. Due to the absence of a transient component in Hung's model, it would predict a uni-phasic decay of vergence in darkness. In both models, the transient component is considered to be non-adaptable. Further, both models assume identical dynamical behavior during convergence and divergence movements (disparity direction or sign independent). The only model that could account for sign

dependent adaptation was proposed by Saladin.[23] This model consists of separate sensorimotor pathways for convergence and divergence. Each pathway is similar to the single pathway proposed by Schor, hence the model has similar predictions related to transient-sustained behavior.

In previous studies, the adaptive changes in the vergence dynamics were only observed under vergence open-loop condition (e.g. in darkness or during monocular viewing) after the adaptation. The vergence decay characteristics in darkness or during monocular viewing were used to determine the effect of adaptation on the sustained component of the vergence system. In order to investigate the effect of adaptation on the behavior of the vergence transient component, in this study, we compare the difference between pre- and post-adaptation short-term closed-loop vergence dynamic responses to a horizontal disparity step at various exposure durations. Further analyses are performed to differentiate the post-adaptation dynamic characteristics during convergence and divergence. In addition, the pre-adaptation dynamic responses are compared to uncover any basic differences between convergence and divergence.

METHODS

Six subjects (LFH, JMW, XHW, VTA, NYN, HNG) participated in this study voluntarily. All the subjects were emmetropic. All had at least 20/20 visual acuity with normal binocular vision. Informed consent was given after the purpose of the experiment was explained to each subject.

Horizontal eye movements of both eyes were measured with a pair of dual Purkinje-image eye-

trackers.[24] In a dark room, using the Badal optical systems attached to the eye-trackers, the subject viewed a pair of bright vertical lines (9 degree in length and 0.35 degree in width; 0.56 cd/sq-m), one presented to each eye on separate monitors with dark background via mirrors positioned in front of the eye-trackers. The stimulus deflection mirrors on the eye-tracker were not used in our experiments. During target viewing, the subject's head movements were restricted by a chin-rest and a fore-head support. A Macintosh II computer controlled the stimulus display and collected data at a sampling rate of 60 Hz per channel, using a 12-bit A/D converter. Two D/A channels were used to map the current stimulus position on each screen. These mapped signals were also recorded along with the eye movement signals. All data were analyzed using the data analysis package AcqKnowledge (BIOPAC Systems Inc.).

The subject initially viewed a target at 4m monocularly through the Badal optical system attached to each eye-tracker. The eye-tracker corresponding to the viewing eye was adjusted such that the visual axis of the subject's eye was closely aligned with the optical axis of the Badal system on the eye-tracker. After the subject's eye had been locked by the eye-tracker, the subject perceived a round aperture and the far target at its center. The same procedure was repeated for the second eye. A rectangular grid was then introduced between the eye and the Badal optical system. The center of the grid was aligned with the optical axis of the Badal system. Then, the 45 deg mirrors to view the computer monitors on which the experimental targets would be presented were set up in front of the eye-trackers. Under the monocular viewing condition, the target presented on the corresponding monitor was adjusted (vertically and horizontally using keyboard) until the subject perceived the center of the target to coincide with the center of the grid. After this alignment procedure was completed for both eyes, the grid was removed from the optical path and the subject was asked to fuse the targets. In case the subject

had vertical phoria, an additional vertical adjustment was performed on one of the two targets until fusion was established. The initial monocular alignment which resulted in binocular viewing at 0 deg (parallel eyes) was fixed during all subsequent sessions. The accommodative demand was held constant at 0 D by placing convex lenses in the optical path of each eye to compensate for the distance of the monitor.

At the start of each experiment, calibration data were collected by using a protocol in which a monocular target at different fixation directions was presented for each eye (other eye is occluded). The eye positions corresponding to the fixation directions were recorded. Then, after a 10 sec delay, the subject was initially exposed to a symmetrical convergence demand of 6 degrees for four different durations: 5s (control), 30s, 60s and 90s. After the stimulus exposure, a square-wave stimulus paradigm was applied. In this paradigm, three 5-s pulses were applied such that the convergence demand toggled between 4 and 6 degrees (see fig. 1a). Three pulses were used for purposes of averaging to improve the signal-to-noise ratio of the vergence signal while minimizing the disturbance to an adapted vergence system. About 10 minutes of rest was introduced between tests at different durations. During the rest time, the subject removed his/her head out of the chin rest and viewed the lighted room normally. In an experiment sequence, the four exposures were tested randomly. Each subject was tested twice, thus providing a maximum of 6 pulses per exposure for subsequent data analysis.

The vergence response was computed by subtracting the two calibrated eye position signals. The signal indicating an eye-blink was also recorded from each eye-tracker. Consistent with observations of Zuber and Stark,[25] Fourier analysis of our vergence step responses indicate a signal attenuation of more than 40 dB around 2 Hz. Therefore, the vergence signal was digitally low-pass filtered at 5 Hz. The

indicator variables used for comparison of transient dynamics are the peak convergence or divergence velocity, the occurrence of peak vergence velocity and the steady-state vergence posture. Since the derivative of a step response is considered to be the characteristic impulse response of a linear system, as a first order approximation, peak vergence velocity computed from small step changes (~ 2 deg) in posture can be a reasonable indicator of the impulse response within a small range.

Figure 1

The vergence velocity signal was computed from the vergence position signal by a two-point backward difference method (ΔT=16.67 msec). A 5 Hz zero-phase FIR filter with 39 coefficients was used. To avoid the ringing due to a sharp edge in the ideal low-pass filter function, a Hamming window was applied to the time-domain coefficients of the ideal low-pass digital filter. The error performance of the derivative algorithm used in this study is comparable to that of the algorithm used by Hung, Zhu & Ciuffreda.[26] Unfiltered responses for which a *saccade* occurred in either eye between the onset of stimulation and 33 msec (2 samples) after a peak vergence velocity occurrence were rejected from further analysis. The criteria used for defining a *saccade* is similar to that used by Zee, Fitzgibbon and Optican.[27] Convergence velocities are positive and divergence velocities are transformed to positive values by negation. As illustrated in fig. 1b, for each subject, the convergence peak velocity (CPV) and divergence peak velocity (DPV) and their corresponding temporal location after stimulus onset (CPL,

DPL) were measured from the vergence velocity signals. The steady-state convergence (SCP) and divergence (SDP) postures were also measured from the vergence position signals. As shown in fig. 1b, SCP and SDP are obtained by averaging the vergence posture of last 2 seconds of the 5 second pulse response. All the parameters (CPV, DPV, SCP, SDP, CPL, DPL) from the three pulses in a single run were averaged to improve the signal-to-noise ratio.

RESULTS

Dynamic vergence data from two subjects (LFH, JMW) are shown in fig. 2. The first two rows show vergence dynamics after different exposure durations. Data from both subjects show an overshoot during divergence after 5 sec exposure duration. Data from LFH showed greater attenuation of the overshoot after 30 sec exposure than the data from JMW. All the subjects showed some amount of overshoot during divergence, although its size was variable. The existence of the overshoot is presumably due to the delay in the vergence control system. That this overshoot was more apparent in divergence responses than convergence responses might be due to the fact that the divergence responses in our data are faster than convergence responses. In contrast, under conditions where convergence velocity is higher than divergence velocity, the convergence response has overshoot.[28] During convergence, a series of smaller steps were observed for both subjects, though it was more prevalent in data from JMW. These smaller steps were absent during divergence. The last two rows show vergence velocity dynamics after different exposure durations. It is clear that the exposure duration has little effect on convergence velocity but for both subjects the divergence velocities after 30, 60 and 90 sec of exposure are lower than the divergence velocity after 5 sec of exposure. The divergence velocity is

greater than convergence velocity for both subjects for all exposure durations.

Figure 2

Comparison of dynamics during divergence and convergence can be better visualized using phase-plane diagrams. The phase-plane technique has been previously used to qualitatively analyze open- and closed-loop vergence dynamics.[29] The phase-plane plots for dynamics during demanded convergence and divergence after 5 and 30 sec duration of exposure for JMW and LFH are shown in fig. 3. For both subjects, the difference in trajectory during demanded divergence after 30 sec of exposure is clearly seen (bottom row). However, the trajectory during a demanded convergence remains relatively unchanged after 30 sec of exposure (top row). The decrease in peak velocity of divergence after 30 sec exposure for both subjects is also evident from the bottom row. The overshoot during divergence movement is illustrated by the corresponding trajectory crossing into the positive velocity area before settling around zero velocity. Divergence overshoot after 30 sec of exposure for LFH shows greater attenuation compared to JMW.

Figure 3

In order to quantitatively analyze the significance of the changes observed in vergence dynamics, characteristic parameters (CPV, DPV, SCP, SDP, CPL, DPL) from all vergence responses were obtained by the measurement technique described in the previous section. A multivariate repeated measures ANOVA (Subject [N=6], Vergence [2 levels] and Exposure [4 levels]) was performed for dependent variables CPV, DPV, CPL and DPL. The Hunyh-Feldt (H-F) p-values were used in all the analysis described in this paper. Out of a total of 236 convergence and divergence responses for all subjects, only 158 were found to be saccade free (previously mentioned criteria) and suitable for further analysis.

Table 1

The average CPV, DPV, CPL, DPL, SCP and SDP from all subjects are shown in fig. 4. In summary, the data in fig. 4 show that the average DPV decreases with increase in exposure duration while the average CPV remains unaltered. The CPL, DPL, SCP and SDP remain unchanged when exposure duration increases from 5 to 90 secs. The average DPV is higher than average CPV for all exposure durations. The results of the repeated measures ANOVA show that the exposure duration significantly affects the vergence velocity ($F[3,15]=6.16$, $p=.006$). There are significant ($F[3,15]=4.52$, $p=.02$) interactions between the direction of vergence movements and the exposure durations indicating that exposure durations differentially affects convergence and divergence. Further analysis shows that the magnitude of the post-exposure (30, 60 and 90 sec) DPV is significantly lower than the control (Table 1, row 1), while the post-exposure CPV does not differ from the control (Table 1, row 2). The average DPV and CPV for different exposure durations is shown in fig. 4a. For all the subjects,

compared to the control condition, there is a consistent reduction in DPV after 30 sec exposure. There is subject dependent variability in DPV after 60 and 90 sec exposure, however on average, the DPV after 60 and 90 sec exposure is lower than the control. Contrary to DPV, as shown in fig. 4a, CPV for all subjects is largely independent of the exposure duration. The differences among average DPV after 30, 60 and 90 sec exposure is nonsignificant (between 30 and 60 sec: $p=0.06$; between 30 and 90 sec: $p=0.28$; between 60 and 90: $p=0.36$).

Figure 4

Table 2

By comparing the pre-task (control, 5 sec) responses of all subjects, the average DPV (10.82 ± 2.29 deg/sec) is significantly (Table 2, row 1, column 1) higher than the average CPV (6.97 ± 1.89 deg/sec). Furthermore, the average DPV remains significantly (Table 2, column 1) higher than the average CPV after all exposure durations. The higher average DPV compared to average CPV is clearly depicted in fig. 4a.

The changes in the average time of occurrence of peak velocity (CPL, DPL) after different exposure durations for both convergence and divergence responses (see fig 4b) were statistically nonsignificant ($F[3,21]=1.66$, $p=.21$). By comparing the pre-task (control, 5 sec) responses of all subjects, the average DPL (.347±.05 sec) is slightly but significantly (Table 2, row 1, column 2) longer than CPL (.314±.039 sec). Furthermore, the average DPL remains slightly but significantly (Table 2, column 2) higher than CPL after all exposure durations. However, note that the differences between CPL and DPL are no more than 2 sampling points. The occurrences of peak velocities are very close to twice the nominal delay (~ 160 msec) seen in the vergence responses, thereby suggesting that CPV and DPV may be occurring at a time very close to the end of the open-loop phase of the vergence responses, which indicates that the effect accommodative interaction might have on the peak vergence velocity can be considered as minimal.

There exists a linear relationship between vergence step demand (instantaneous disparity) and peak vergence response velocity.[34] Hence the results obtained for vergence velocities after different exposures could be explained by corresponding changes in the vergence step demand. A change in vergence step demand could be caused if the steady-state postures after various exposure durations are different, possibly due to a significant reduction in steady-state errors. To rule out such a possibility, multivariate repeated measures ANOVA (Subject [N=6], Vergence [2 levels], Exposure [4 levels]) was performed for dependent variable steady-state vergence posture (SCP, SDP). The effect of exposure duration on steady-state vergence posture ($F[3,15]=1.1$, $p=.38$) was nonsignificant. In fact as expected, most of the variation in the ANOVA model were explained by the type (6 deg or 4 deg) of vergence posture ($F[1,5]=467.9$, $p=.0001$). This suggests that the alteration of divergence dynamics was a result of a vergence system change and did not merely reflect a change in vergence step demand. The average

SCP and SDP after different exposure durations are shown in fig. 4c.

DISCUSSION

The main finding of this study is that the transient component of the horizontal disparity vergence system is altered after sustained convergence. Such alteration can be viewed as an adaptation phenomenon observed when the vergence system is operating in closed-loop. Existing vergence adaptation models cannot explain this phenomenon based on changes in tonic vergence posture. At the vergence posture tested, only the divergence dynamics showed adaptive effects. The nature of the adaptation process is illustrated in fig. 5.

Figure. 5

Because the change in convergence velocity is negligible and is not equal to the change predicted by a linear process (see fig. 5), the adaptation process reported here is non-linear. Further, the adaptive phenomenon is also non-linear with respect to the duration that induces it. The nature of adaptation might vary if testing were performed at different adapting postures, but the present tests are sufficient to uncover the basic non-linear adaptive nature of the transient component in the vergence system. Additional tests at other postures and with other amplitudes would enhance the characterization of the adaptive phenomenon reported here. The role of adaptation within the transient component is not very

clear. Static analysis of the dynamic neural network vergence model[35] suggests that the steady-state vergence error is related to the ratio of convergence and divergence peak velocities, with the error approaching zero if the ratio is unity. Some of the data are consistent with the static analysis of the model from a standpoint that the magnitude of peak divergence velocity is tending towards convergence velocity in the first 30 seconds thereby reducing the asymmetry in the dynamics. Due to the amplitude resolution limitation of the eye trackers, a reduction in steady-state error is not evident in the data presented here.

The short-term vergence dynamics after sustained convergence have not been correctly predicted by the current vergence adaptation models.[21-23] Even though the adaptation process is modeled differently in these models (recruitment mechanisms in Schor's and Saladin's model and time-constant modulation in Hung's model), all the models suggest the short-term closed-loop responses are unaffected by adaptation - a prediction we have shown to be false in this study. Since most models do not discriminate between convergence and divergence except by a sign, they are also unable to predict any difference in dynamics between them. Further, none of the above models has been tested with a wide range of open and closed-loop stimulus conditions.

The recent neural network model[35] has been used to explain a wide range of short-term vergence dynamics. However, this model currently does not include any time-dependent adaptive components. In this model, one possible neural site for a rapid adaptation is the vergence velocity cells.[5] However the adaptation at this site has to be accomplished by interactions between the divergence and convergence velocity cells. One possible way would be to compare the steady-state firing rates of the convergence and divergence velocity cells and then to inhibit the cells that have a higher rate. The inhibition would

be proportional to the difference in the steady-state firing rates of the convergence and divergence velocity cells. The entire compare-and-control circuit would have a *time-constant* of about 6 seconds thus causing total adaptation in about 30 seconds. Once the adaptation process has settled, further exposure to the adapting stimulus would not alter the adapted system.

The values of CPL and DPL are useful in eliminating the possibility that the peak vergence velocities reported here were affected by accommodative interactions. Since the accommodative loop was not opened, the interactions between the vergence and the accommodation system can cause an effect on the vergence dynamics.[30-32] If CPV and DPV were influenced by *accommodative vergence signal resulting from changes in vergence demand* (AC/V), then they would not be appropriate characteristic parameters for the vergence system. However, the AC/V signal has to travel via the vergence-to-accommodation (CA) cross link, the accommodative feedback, and the accommodation-to-vergence (AC) cross link before affecting the vergence dynamics.[22] The latency between the onset of an accommodative stimulus and the resulting vergence change is approximately 250 msec.[33] It is also unlikely that the CA cross link originates and terminates without a significant delay. Assuming the CA cross link latency of about 150 msec (half the total of 300 msec[22]), the elapsed time before the first interaction of the AC/V signal with the vergence signal is 400 msec. In the worst case, the vergence velocity (DPL) reaches its peak at about 350 msec, hence there is little probability that the AC/V signal due to the constant accommodation demand directly influences the CPV and DPV values. This issue should however not be confused with the issue discussed in the following paragraph regarding the effect that steady-state accommodation could have on vergence dynamics.

Near the 6 deg vergence posture that was used for testing in this paper, the average divergence

velocity was significantly higher than average convergence velocity. Idiosyncratic comparison results have been reported by several researchers.[25-28,36,37] Zuber and Stark,[25] Krishnan and Stark,[28] Hung et al.[26] and Zee et al.[27] have reported that convergence velocity is higher than divergence velocity. Schor et al.[36] and Erkelens et al.[37] have reported both conditions. In our experiments, we believe that one of the reasons for divergence being faster than convergence is due to the accommodation demand being held constant at 0D. Considering the synergy between the accommodation and the vergence system, accommodation would have a tendency to facilitate (inhibit) vergence that is in the direction consistent (inconsistent) with itself. The magnitude of convergence and divergence velocities may also depend on the vergence posture tested. Simulations of the neural network model of horizontal disparity vergence[35] predict such a posture dependent non-linearity in the vergence system. Due to the interactions between the accommodation and the vergence system, the accommodative vergence through the crosslinks[22] would affect the internal vergence signal needed to obtain a given demanded vergence posture. The demanded vergence posture is obtained by adding the internal vergence signal with the accommodative vergence signal. Hence accommodative posture used for testing would also influence the comparison between divergence and convergence peak velocities. Another factor that could determine the relationship between vergence velocity and vergence posture is dark vergence. Both accommodative vergence and dark vergence would act as biases to set the internal operating points of the convergence and divergence position integrators. In fact, it is highly likely that convergence peak velocity would be higher than divergence peak velocity for a range of vergence postures if the accommodation is allowed to vary synergetically with the vergence response or if the dark vergence is comparably higher. So while the difference between convergence and divergence velocities clearly stress the need for separate consideration, the magnitude and sign of such a difference must be carefully evaluated.

In summary, the transient component in the horizontal disparity system adapts. Evidence is presented for an adaptation phenomenon that is observed while the vergence system is operating in a normal closed-loop mode. The adaptation is rapid and is shown to be non-linear with respect to convergence and divergence and the duration that induces it. At the accommodation demand and vergence posture tested, there are significant differences in the dynamics during convergence and divergence as indicated by differences in magnitudes of peak velocities and their occurrence times pre- and post-adaptation. These results also suggest that separate pathways for convergence and divergence are involved in vergence sensorimotor control.

ACKNOWLEDGMENTS

This study was supported in part by NIH grants EY08862, MH49892, Texas Advanced Technology Program under grant 003652023 and University of Houston ISSO. We thank Dr. Harold Bedell for his valuable discussions and comments on the manuscript. We also thank all the subjects for their valuable time and effort.

REFERENCES

1. Maddox EE. The clinical use of prism; and the decentering of lenses. 2nd ed. Bristol, England: John Wright & Sons, 1893.
2. Schor CM, Horner D. Adaptive disorders of accommodation and vergence in binocular dysfunction. Opthal Physiol Opt 1989; 9: 264-268.
3. Owens DA, Leibowitz HW. Perceptual and motor consequences of tonic vergence. In Schor CM. & Ciuffreda KJ. (Eds), Vergence eye movements: Basic and clinical aspects (pp. 25-72). London: Butterworths, 1983.
4. Mays LE. Neural control of eye movements: convergence and divergence neurons in midbrain. Journal of Neurophysiology 1984; 51: 1091-1108.
5. Mays LE, Porter JD, Gamlin PDR, Tello CA. Neural control of vergence eye movements: neurons encoding vergence velocity. Journal of Neurophysiology 1986; 56: 1007-1021.
6. Schor CM. The influence of rapid prism adaptation upon fixation disparity. Vision Research 1979; 19: 757-765.
7. Sethi B. Vergence adaptation: a review. Documenta Ophthalmologica 1986; 63: 247-263.
8. Ellerbrock VJ. Tonicity induced by fusional movements. American Journal Optometry and Archives of American Academy of Optometry 1950; 27: 8-20.
9. Carter DB. Fixation Disparity and Heterophoria Following Prolonged Wearing of Prisms. Am J Optom Arch Am Acad Optom 1965; 42: 141-152.
10. Henson DB, North R. Adaptation to Prism-Induced Heterophoria. Am J Optom Physiol Opt 1980;

57: 129-137.

11. Miles FA, Judge SJ, Optican LM. Optically Induced Changes in the Couplings Between Vergence and Accommodation. J Neuroscience 1987; 7: 2576-2589.

12. Schor CM. Analysis of Tonic and Accommodative Vergence Disorders of Binocular Vision. American Journal of Optometry & Physiological Optics 1983; 60: 1-14.

13. Owens DA, Wolf-Kelly K. Near Work, Visual Fatigue, and Variations of Oculomotor Tonus. Investigative Opthalmology & Visual Science 1987; 4: 743-749.

14. Wolf KS, Ciuffreda KJ, Jacobs SE. Time Course and Decay of Effects of Near Work on Tonic Accommodation and Tonic Vergence. Opthal Physiol Opt 1987; 7: 131-135.

15. Rosenfield M, Gilmartin B. Accommodative Adaptation Induced by Sustained Disparity-Vergence. American Journal of Optometry and Physiological Optics 1988; 65: 118-126.

16. Fisher SK, Ciuffreda KJ, Bird JE. The Effect of Stimulus Duration on Tonic Accommodation and Tonic Vergence. Optometry and Vision Science 1990; 67: 441-449.

17. Cooper J. Clinical Implications of Vergence Adaptation. Optometry and Vision Science 1992; 69: 300-307.

18. Ciuffreda KJ, Hung GK. Symptoms Related to Abnormal Tonic State: Experimental Results and Computer Simulations. Optometry and Vision Science 1992; 69: 283-288.

19. Carniglia PE, Cooper J. Vergence Adaptation in Esotropia. Optometry and Vision Science 1992; 69: 308-313.

20. Morley W, Judge SJ, Lindsey JW. Role of Monkey Midbrain Near-Response Neurons in Phoria Adaptation. Journal of Neurophysiology 1992; 67: 1475-1492.

21. Hung GK. Adaptation model of accommodation and vergence. Ophthalmic & Physiological Optics 1992; 12: 319-326.

22. Schor CM. A dynamic model of cross-coupling between accommodation and convergence: simulations of step and frequency responses. Optometry and Vision Science 1992; 69: 258-269.

23. Saladin JJ. Convergence Insufficiency, Fixation Disparity, and Control System Analysis. American Journal of Optometry & Physiological Optics 1986; 63: 645-653.

24. Crane HD, Steele CM. Accurate Three-Dimensional Eyetracker. Applied Optics 1978; 17: 691-705.

25. Zuber BL, Stark L. Dynamical Characteristics of the Fusional Vergence Eye-Movement System. IEEE Trans on Systems Science and Cyber 1968; SSC-4: 72-79.

26. Hung GK, Zhu HM, Ciuffreda KJ. Convergence and divergence exhibit different response characteristics to symmetric stimuli. Vision Research 1997; 37: 1197-1205.

27. Zee DS, Fitzgibbon EJ, and Optican LM. Saccade-Vergence Interactions in Humans. Journal of Neurophysiology 1992; 68: 1624-1641.

28. Krishnan VV, Stark L. A heuristic model for the human vergence eye movement system. IEEE Transactions on Biomedical Engineering 1977; 24, 44-49.

29. Semmlow JL, Hung GK, Horng JL, Ciuffreda KJ. Disparity Vergence Eye Movements Exhibits Preprogrammed Motor Control. Vision Research 1994; 34: 1335-1343.

30. Mueller J. Elements of Physiology, Vol. 2. Baly W, trans. London: Taylor and Walton, 1826.

31. Alpern M, Ellen P. A quantitative analysis of the horizontal movements of the eyes in the experiments of Johannes Mueller. I. Methods and Results. Am J Opthal 1956; 42: 289-303.

32. Semmlow JL, Venkiteswaran N. Dynamic Accommodative Vergence in Binocular Vision. Vision Research 1976; 16: 403-411.

33. Wilson D. A centre for accommodative vergence motor control. Vision Research 1973; 13: 2491-2503.

34. Rashbass C, Westheimer G. Disjunctive Eye Movements. Journal of Physiology 1961; 159: 339-360.

35. Patel SS, Ogmen H, White JM, Jiang B. Neural network model of short-term disparity vergence dynamics. Vision Research 1997; 37: 1383-1399.

36. Schor CM, Robertson KM, Wesson M. Disparity vergence dynamics and fixation disparity. American Journal of Optometry & Physiological Optics 1986; 63: 611-618.

37. Erkelens CJ, Van der Steen J, Steinman RM, Collewijn H. Ocular vergence under natural conditions I. Continuous changes of target distance along median plane. Proc R Soc Lond 1989; B236: 417-440.

Bai-Chuan Jiang

College of Optometry

University of Houston

Houston, TX 77204-6052

BJiang@uh.edu

FIGURE AND TABLE LEGENDS

Figure 1. Stimulus protocol and characteristic parameters used in our experiments. (a) The protocol used for the sustained convergence experiments. The symmetric convergence demand is created by simultaneously translating half the required vergence demand as monocular nasal shift for each eye. The numbers (5, 10, 90) indicate various exposure durations at a given demand. The arrow represents the variable exposure duration (5, 30, 60 or 90 sec). (b) The top row shows a section of the stimulation paradigm in our experiment containing a 2 deg pulse (from 6 deg to 4 deg). The middle row shows the vergence response during the pulse section. The average steady-state convergence posture (SCP) is obtained by averaging the vergence position data from the last 2 seconds for a 6 deg vergence stimulus. Similarly, SDP is the average steady-state vergence posture for a 4 deg stimulus. Upward (downward) deviation in this trace and in following figures indicates increased convergence (divergence). The bottom row shows the corresponding vergence velocity trace. The negative peak (DPV) corresponds to the peak velocity during 2 deg divergence. The positive peak (CPV) corresponds to the peak velocity during 2 deg convergence. The occurrence of these peaks are marked by a vertical line. The durations between stimulus transition and the location of the corresponding velocity peaks (DPL and CPL) are indicated by arrows.

Figure 2. Vergence dynamics as a function of exposure duration for two subjects (a. JMW, b. LFH). The exposure durations are indicated in the top row. The point of stimulation corresponds to the left edge of each rectangle. The vergence position, vergence velocity and time scales are identical for both subjects and are shown in the respective left columns. The top row shows convergence dynamics and the row below shows divergence dynamics. The bottom row shows divergence velocity dynamics

and the row above shows convergence velocity dynamics.

Figure 3. Phase-plane trajectories of convergence and divergence dynamics for two subjects (JMW, LFH). Unfilled (filled) symbols represent dynamics after 5 (30) sec. The square (circle) symbols represent dynamics in response to a convergence (divergence) demand (2 deg). Positive (negative) vergence velocity represents convergence (divergence) movement. For this and all subsequent figures, the error bars represent standard error.

Figure 4. Various average vergence parameters and their relationship with exposure duration. (a) Average convergence and divergence peak velocities (CPV, DPV). (b) Average convergence and divergence peak velocity occurrence time (CPL, DPL). (c) Average steady-state convergence and divergence postures (SCP, SDP).

Figure 5. The relationship between disparity step and the corresponding peak vergence velocity. In order to show that the vergence adaptation process is non-linear, some of the data from 4a are replotted in this figure. On the x-axis, negative and positive values correspond to uncrossed and crossed disparity steps, respectively. On the y-axis, negative and positive values correspond to divergence and convergence velocities, respectively. The point on the origin is an 'implicit' data point that represents zero velocity or no movement when the disparity does not change. The pre- adaptation data points are plotted with square symbols and the post- adaptation data points, which correspond to the data points for an adaptation duration of 30 sec in figure 4, are plotted with diamond symbols. The divergence velocity is reduced by a factor of about 1.3 after the adaptation. If the adaptation process were linear, we would predict that the convergence velocity after the adaptation will be reduced by the same factor, which is

shown by the point with an open circle symbol. However, the result shows that the adaptation does not change the convergence velocity as per this prediction.

Table 1. Statistical comparisons of average CPV and DPV. Comparisons are between the average DPV and CPV (N=6) after exposure durations in each column with the corresponding values after exposure of 5 sec (control).

Table 2. Statistical comparisons between average CPV and DPV, and, average CPL and DPL (N=6), after different convergence exposure.

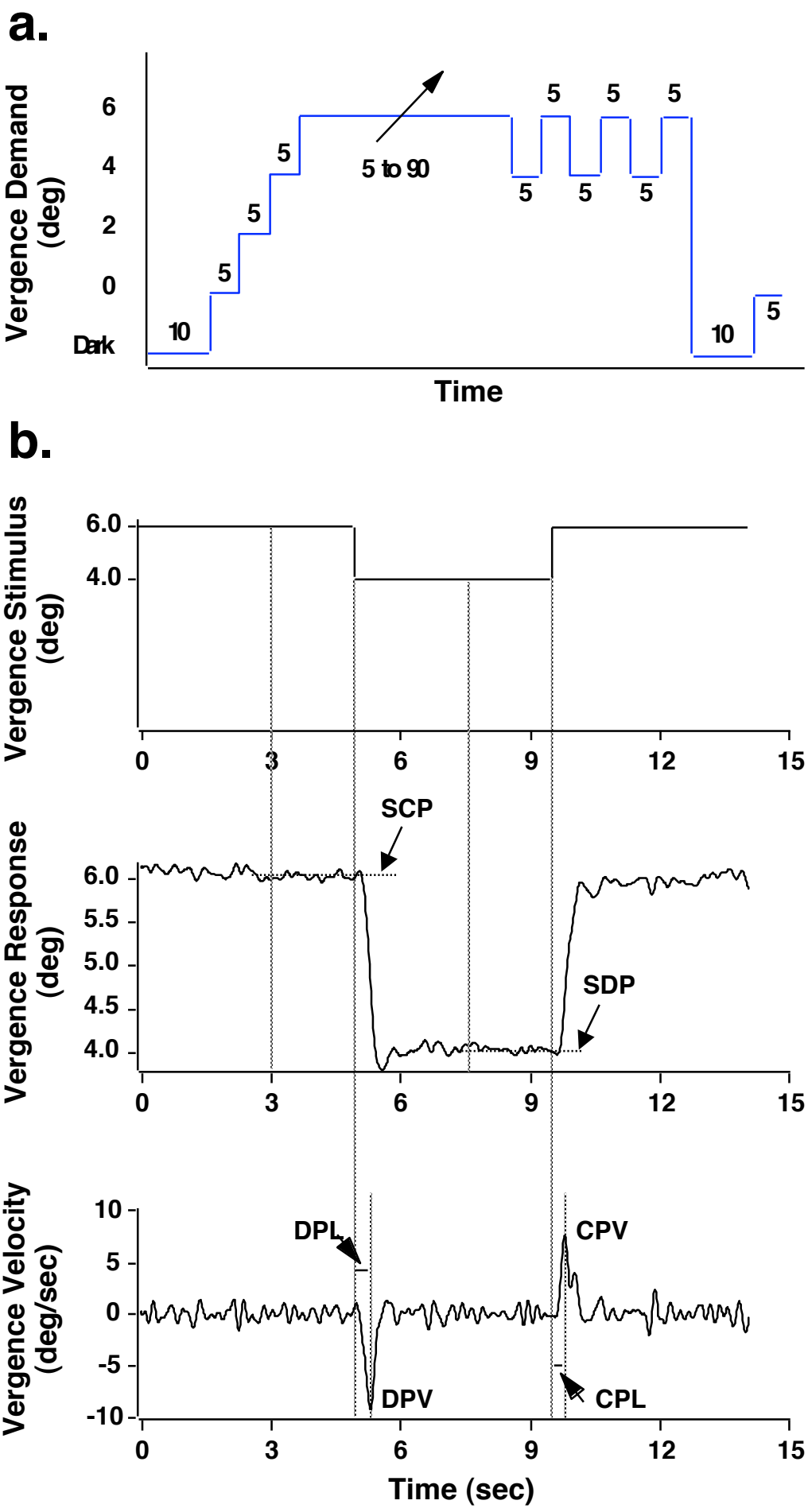
a.
Vergence Demand (deg)
6
4
2
0
Dark
10
5
5
5
5
5 to 90
5
5
5
5
5
5
10
5
Time
b.
Vergence Stimulus (deg)
6.0
4.0
0
3
6
9
12
15
Vergence Response (deg)
SCP
SDP
6.0
5.5
5.0
4.5
4.0
Vergence Velocity (deg/sec)
DPL
DPV
CPV
CPL
10
5
0
-5
-10
Time (sec)

Figure 1

Figure 2

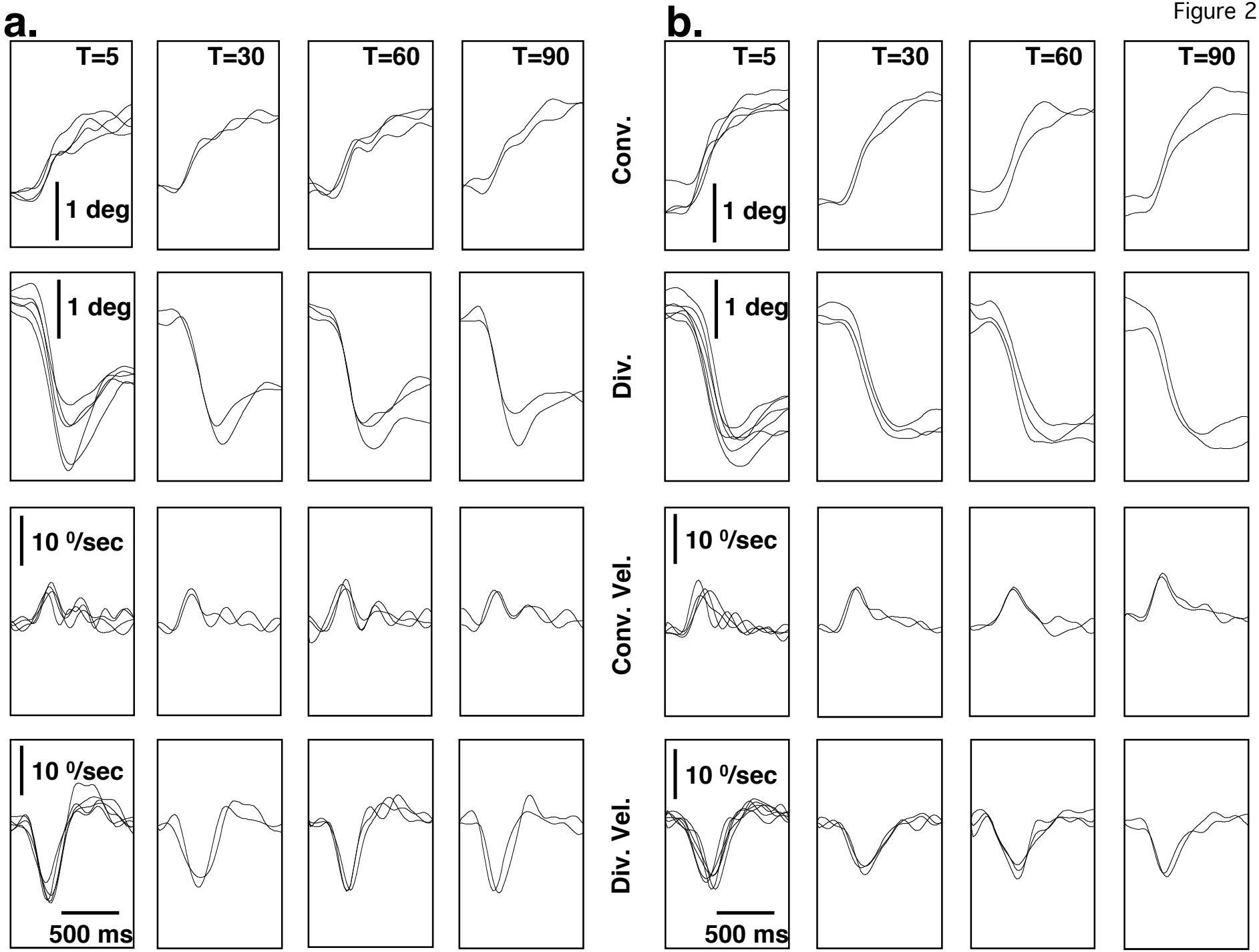

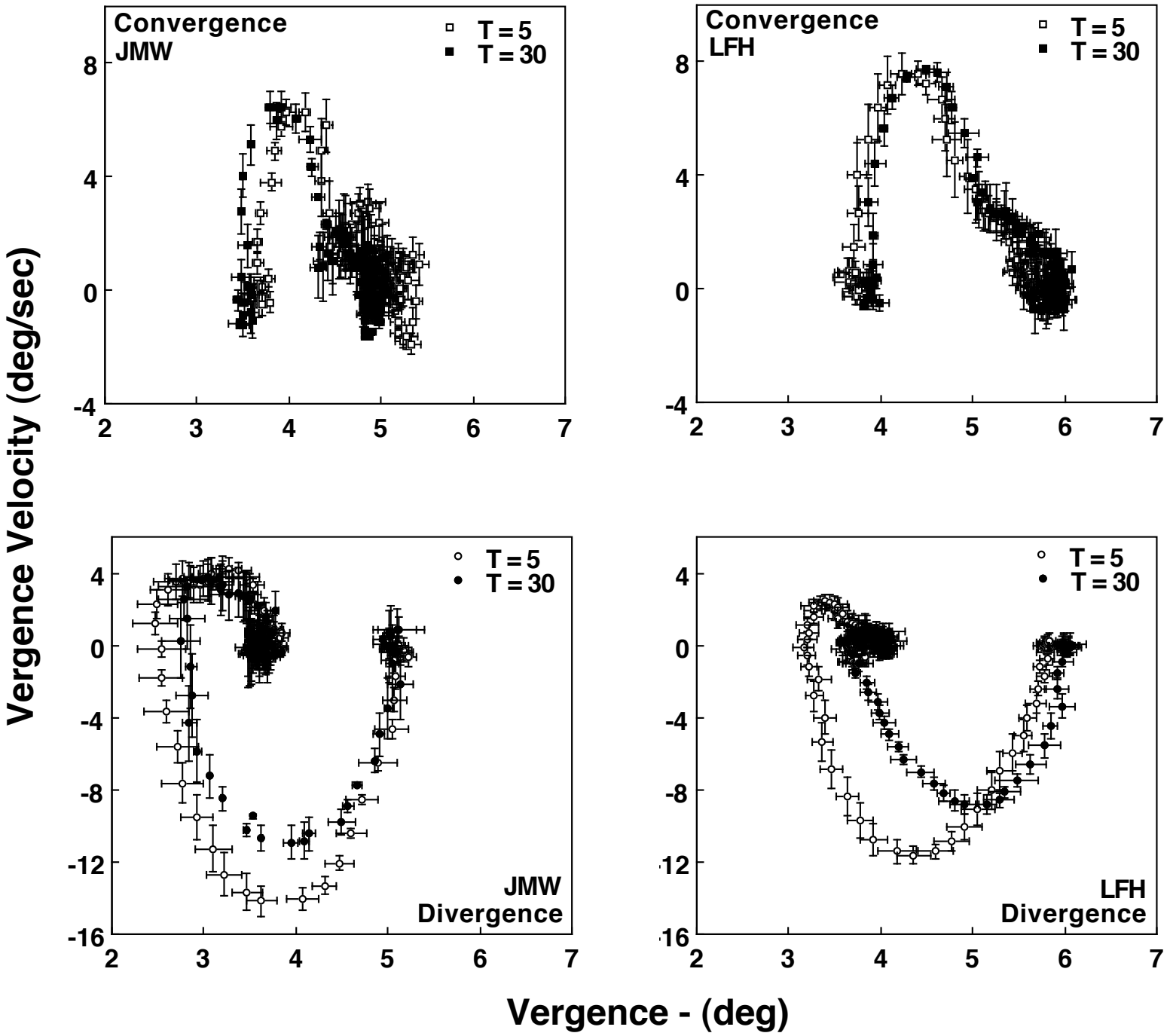
Convergence
JMW
T = 5
T = 30
Convergence
LFH
T = 5
T = 30
T = 5
T = 30
JMW
Divergence
T = 5
T = 30
LFH
Divergence
Vergence Velocity (deg/sec)
Vergence - (deg)

Figure 3

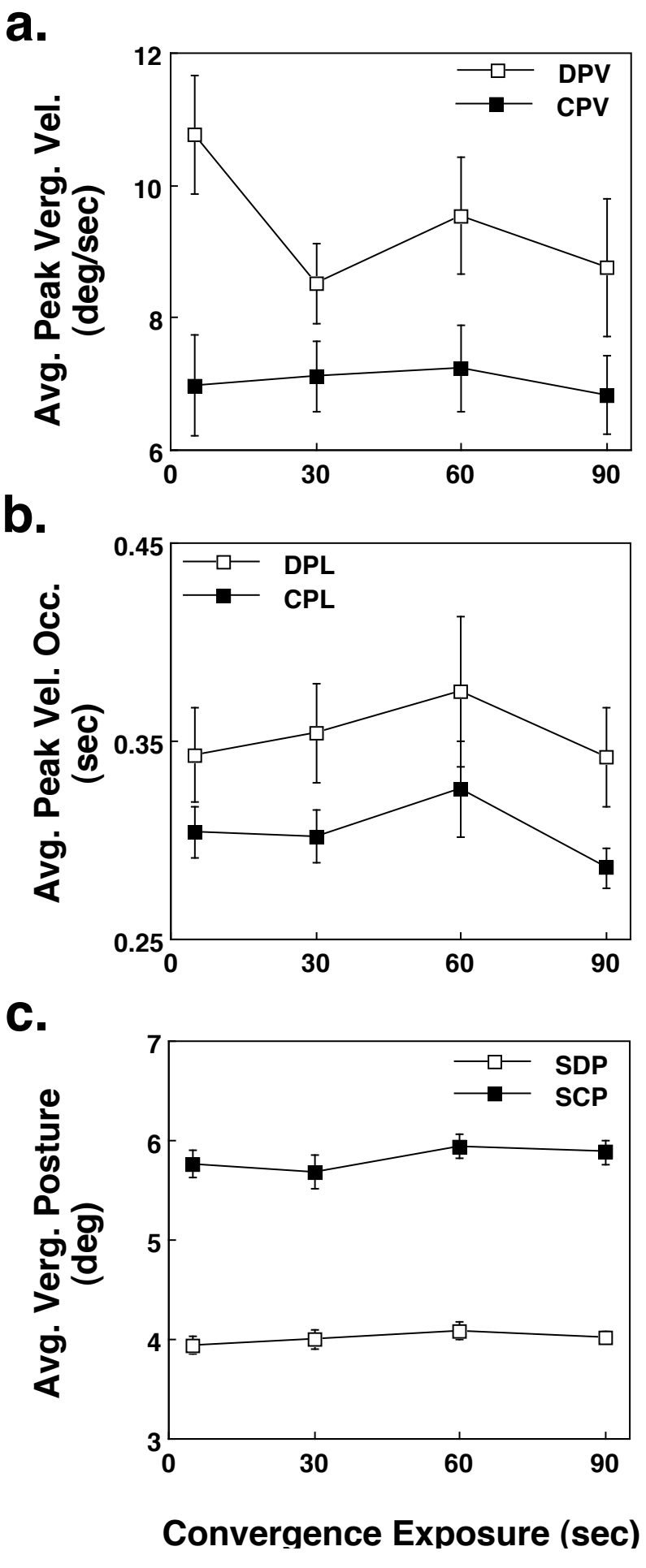
a.
Avg. Peak Verg. Vel. (deg/sec)
12
10
8
6
DPV
CPV
0
30
60
90
b.
Avg. Peak Vel. Occ. (sec)
0.45
0.35
0.25
DPL
CPL
0
30
60
90
c.
Avg. Verg. Posture (deg)
7
6
5
4
3
SDP
SCP
0
30
60
90
Convergence Exposure (sec)

Figure 4

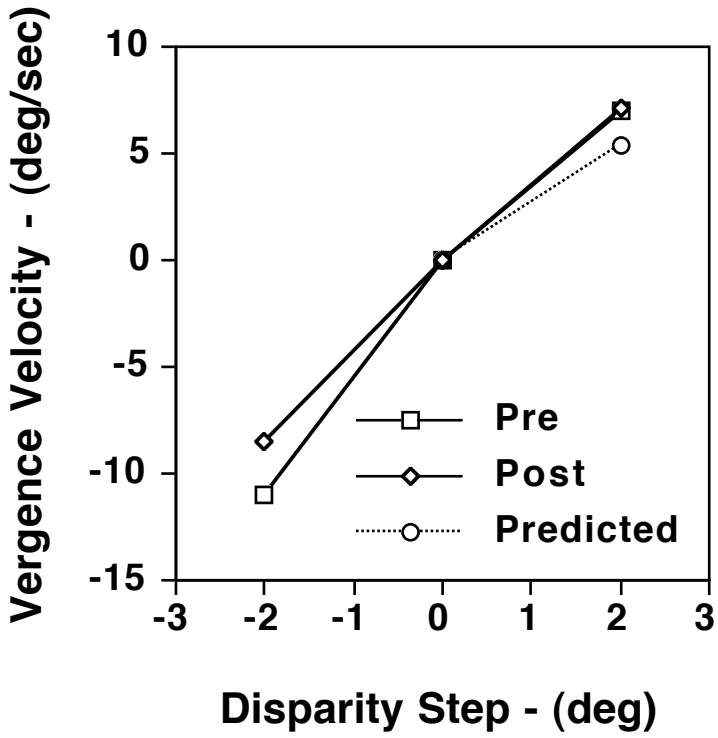
Vergence Velocity - (deg/sec)
10
5
0
-5
-10
-15
-3
-2
-1
0
1
2
3
Pre
Post
Predicted
Disparity Step - (deg)

Figure 5

Table 1.

	30 sec	**60 sec**	**90 sec**
DPV	F[1,15]=21.97 p=.0004	F[1,15]=6.54 p=.02	F[1,15]=17.46 p=.001
CPV	F[1,15]=.07 p=.78	F[1,15]=.27 p=.6	F[1,15]=.1 p=.74

Table 2.

	DPV v/s CPV	**DPL v/s CPL**
5 sec	F[1,21]=54.6 p=.0001	F[1,21]=5.28 p=.03
30 sec	F[1,21]=17.89 p=.001	F[1,21]=4.2 p=.05
60 sec	F[1,21]=12.89 p=.003	F[1,21]=6.79 p=.02
90 sec	F[1,21]=10.7 p=.006	F[1,21]=14.1 p=.001